Improved differentiation of NPS analogs through the application of chemometric methods to GC-solid deposition-FTIR spectra

Bonetti, J.L.; Kranenburg, R.F.; Hokanson, S.; Pothier, M.; Samanipour, S.; van Asten, A.C.

DOI
10.1016/j.forc.2024.100619

Publication date
2024

Document Version
Final published version

Published in
Forensic Chemistry

License
CC BY

Forensic Chemistry 41 (2024) 100619

Contents lists available at ScienceDirect

Forensic Chemistry

journal homepage: www.sciencedirect.com/journal/forensic-chemistry

Improved differentiation of NPS analogs through the application of chemometric methods to GC-solid deposition-FTIR spectra

Jennifer L. Bonetti [a,b,*], Ruben F. Kranenburg [a,c], Stephen Hokanson [b,e], Matthew Pothier [e], Saer Samanipour [a,f,g,h], Arian C. van Asten [a,d]

[a] Van't Hoff Institute for Molecular Sciences, University of Amsterdam, P.O. Box 94157, Amsterdam 1090 GD, The Netherlands
[b] Virginia Department of Forensic Science, Norfolk, VA 23510, USA
[c] The Netherlands Police, Unit National Expertise and Operations (LX), Domain R&D, Innovation and Expertise (RiX), National Forensic Service Center, Postbus 100, Driebergen 3970 AC, The Netherlands
[d] Co van Ledden Hulsebosch Center (CLHC), Netherlands Center for Forensic Science and, Medicine, 1098 XH Amsterdam, The Netherlands
[e] Virginia Department of Forensic Science, Roanoke, VA 24019, USA
[f] Centre for Analytical Sciences Amsterdam, Amsterdam, the Netherlands
[g] UvA Data Science Centre, University of Amsterdam, Amsterdam, the Netherlands
[h] Queensland Alliance for Environmental Health Sciences (QAEHS), The University of Queensland, Woolloongabba, Australia

ARTICLE INFO

Keywords:
Forensic science
Drug analysis
Novel psychoactive substances
Chemometrics
Gas chromatography
Infrared spectroscopy

ABSTRACT

Novel psychoactive substances pose a significant analytical challenge for forensic laboratories. Gas Chromatography with Infrared Spectroscopy (GC-IR) is typically presented as producing visually distinct spectra. However, this is not the case for all compounds. In this study, we showcase three synthetic cathinone analogs (methylone, N-ethylpentylone, and pentylone) which produce extremely visually similar solid state IR spectra.

A primary dataset of these analogs was generated at the Amsterdam Police Laboratory. Libraries were created using two different sample preparation methods. The same compounds were also analyzed at the Virginia Department of Forensic Science (DFS). It was observed that changes in either instrument or sample preparation were enough to pose challenges to both the visual assessment and a library matching algorithm. Additionally, week-to-week variation was observed within the primary dataset. Principal Component Analysis (PCA) in combination with mahalanobis distances for objective comparison was assessed. A leave-one-sample-out cross validation accurately identified 100% of the samples in the primary dataset.

This study shows how the application of chemometrics to spectral GC-IR data can substantiate the instrument's differentiation capabilities and provide valuable objective support for a compound identification. In addition, limitations in the consistency of GC-IR spectra over time and across instruments and sample preparation methods were observed which could affect how the forensic community utilizes these techniques. Specifically, this study shows that shared GC-IR libraries might pose selectivity limitations. Therefore, laboratories must exercise caution if shared/generic GC-IR libraries are utilized for casework, and it is recommended that instrument and solvent specific libraries are generated.

Introduction

The field of forensic illicit drug analysis has long considered Gas Chromatography/Mass Spectrometry (GC–MS) to be the gold standard of available instrumental methods due to the combination of the separation capabilities provided by chromatography, coupled with the structural information generated by the mass spectrometer. However, new compounds have been entering the drug market at a staggering rate, creating analytical challenges for forensic laboratories. In 2021, the cumulative number of novel psychoactive substances (NPSs) identified during the preceding fifteen year timespan reached 1165 globally [1]. With so many new, often structurally similar, compounds being encountered across the drug landscape, GC–MS data does not always suffice for confident identification. Substantial research into new analytical strategies and instrumental methods has been conducted in an effort to address these limitations [2].

* Corresponding author at: Virginia Department of Forensic Science, Norfolk, VA 23510, USA
E-mail address: J.L.Bonetti@uva.nl (J.L. Bonetti).

https://doi.org/10.1016/j.forc.2024.100619
Received 23 August 2024; Received in revised form 29 October 2024; Accepted 1 November 2024
Available online 14 November 2024

Although many spectroscopic techniques are available that provide structural characterization to complement the information generated by the mass spectrometer, they typically require a level of purity not commonly encountered in most drug exhibits. Thus, the combination of gas chromatography with various spectroscopic methods has been extensively studied, as discussed in a thorough review by Aslani and Armstrong [3]. These spectroscopic methods include fourier transform infrared spectroscopy (FTIR), nuclear magnetic resonance spectroscopy (NMR), vacuum ultraviolet spectroscopy (VUV), and molecular rotational resonance spectroscopy (MRR).

FTIR has been employed in many forensic applications [4–6], so it is logical that the combination of gas chromatography with both vapor-phase and solid-deposition FTIR spectroscopy has been proposed as an alternative technique for situations where chromatographic separation is necessary, but mass spectrometry alone is insufficient for structural differentiation of similar compounds [7–12].

There have been many studies reporting on the success of GC-IR techniques for identifying and differentiating a myriad of challenging drugs of abuse, such as fentanyl analogs [9], positional isomers of fentanyl related substances [11], isomeric ethoxyphenethylamines and methoxymethcathinones [13], substituted benzylpiperazine isomers [10,14], phenylisopropylamines [15] regioisomeric phenethylamines [8], and others [16–20]. The importance of these studies is commonly predicated on the use of compounds that produce similar mass spectra. Due to the complementary nature of mass spectrometry and infrared spectroscopy, substances that produce visually similar mass spectra, such as positional isomers and diastereomers, will typically generate distinct infrared spectra [7]. In addition, the reverse relationship typically holds true. Substances which produce visually similar infrared spectra will typically generate distinguishable mass spectra [7], illustrating the high degree of orthogonality of the combination of infrared spectroscopy and mass spectrometry. Most of the studies comparing infrared spectra of isomers are relying on visual spectral comparison which may be sufficient for spectra with substantial discrepancies, but additional objective tools are necessary when spectra are visually similar [21].

While the combination of multiple orthogonal analytical methods is typically preferred, there could be situations where only one instrumental technique is available. Thus, it is important to establish whether statistical or chemometric analysis of the generated data could feasibly be applied to enhance the differentiation capabilities of the available method.

For example, previous work has shown that statistical methods such as Principal Component Analysis (PCA) and/or Linear Discriminant Analysis (LDA) can be utilized to successfully differentiate between positional isomers based on visually identical electron ionization mass spectra [22–26], VUV spectra [27], Raman spectra [28], and even mass spectral data produced via Direct Analysis in Real Time/Time-of-Flight Mass Spectrometry [29].

A recent review highlighted the promising combination of chemometrics with infrared spectroscopy for forensic drug analyses [30]. Many of the discussed applications focused on field analyses, such as those occurring at borders or drug-checking sites, where a rapid screening technique is desired, in contrast to a full laboratory analysis. Most of the chemometric models were developed for quick cocaine base determination, purity estimation, or improved screening results of impure samples in the absence of a time-consuming chromatographic analysis. While most of the studies utilized portable instrumentation, there were some which incorporated a GC-IR set-up. Typically, the methods were proposed as screening techniques for drug class determination rather than as a means of confirming the identity of the compounds [31–34]. To the best of the authors' knowledge, no work has yet been published that investigates the application of chemometrics to GC-IR data of NPSs for the purpose of enhancing the confidence of the final identification.

The purpose of this study was to assess the feasibility of using chemometrics to improve the objective comparison of visually similar GC-IR spectra using solid deposition. A primary dataset made up of replicate spectra of three synthetic cathinones was utilized to create a chemometric training dataset. Using that dataset, PCA was used to identify the axes that best represent the variance in the data. In this unsupervised manner, any natural differences in the spectra can be highlighted without overfitting the model as may occur with a supervised model such as LDA. Subsequently, the ability of the model to objectively identify spectra from test sets made up of reference standards from two different laboratories and sample preparation methods, case samples, and cathinones not included in the primary dataset was assessed. In doing so, valuable information was obtained on the robustness and reproducibility of IR spectral data as produced with GC-solid deposition-IR.

Materials and methods

Reagents and materials

The primary dataset for this study was prepared at the Amsterdam Police Laboratory (APL). Reference materials of 3,4-methylenedioxymethcathinone HCl (methylone) and 1(1,3-benzodioxol-5-yl)-2-(ethylamino)-1-pentanone HCl (N-ethylpentylone) at this laboratory originated from high-purity seized materials whose identities were confirmed by GC–MS, FTIR, and Raman methods. In addition, *β*-keto-methylbenzodioxolyl-pentanamine HCl (pentylone) was obtained using casework material which was identified according to the laboratory's validated analysis methods (GC–MS). Chloroform (analysis grade), methanol (chromatography grade), demineralized water (pure), and sodium hydroxide monohydrate (>99 %) were obtained from VWR Avantor (Radnor, PA, USA). Additional cathinone reference spectra were investigated, but these three cathinone analogs were found to produce the most visual spectral similarity and were thus selected to form the primary dataset.

The first test set originated from APL and consisted of realistic forensic case samples from the greater Amsterdam area. Case sample 1 was an orange Armani-logo shaped tablet, and Case sample 2 was an off-white powder. These case samples were different from the casework samples utilized to prepare the previously mentioned reference samples.

A secondary test set was generated at the Virginia Department of Forensic Science (DFS) at the western regional laboratory to assess the robustness of the chemometric model to data generated using different instrumentation. In addition to the three compounds included in the primary dataset, other cathinones which were considered likely to produce similar spectra were analyzed including 3,4-methylenedioxyethcathinone (ethylone), *β*-keto-N-methyl-3,4-benzodioxolylbutanamine (butylone), 1-(1,3-benzodioxol-5-yl)-2-(ethylamino)-1-butanone (eutylone), 3,4-Methylenedioxy-*α*-methylaminohexanophenone (N-methylhexylone), as well as the 2,3- positional isomers of both methylone and pentylone. The structures for all cathinones utilized in this study are shown in Fig. 1. Primary standards from Cayman Chemical (Ann Arbor, MI) were used for all DFS analyses with the exception of N-ethylpentylone and ethylone which were secondary standards acquired from case samples. The identity of the N-ethylpentylone sample was confirmed via Attenuated total Reflectance (ATR), Gas Chromatography-Flame Ionization Detector-Mass Spectrometry (GC-FID-MS) and GC-IR, while the ethylone sample was verified using GC-FID-MS. The structure of Nethylpentylone provides more isomeric possibilities than that of ethylone which is why additional characterization was performed. In both instances, the data was compared to that generated using a primary standard. Chloroform and methanol (both HPLC grade) used at this laboratory were obtained from Fisher Chemical (Pittsburgh, PA), and sodium hydroxide pellets (97 %) were obtained from Acros Organics (Belgium).

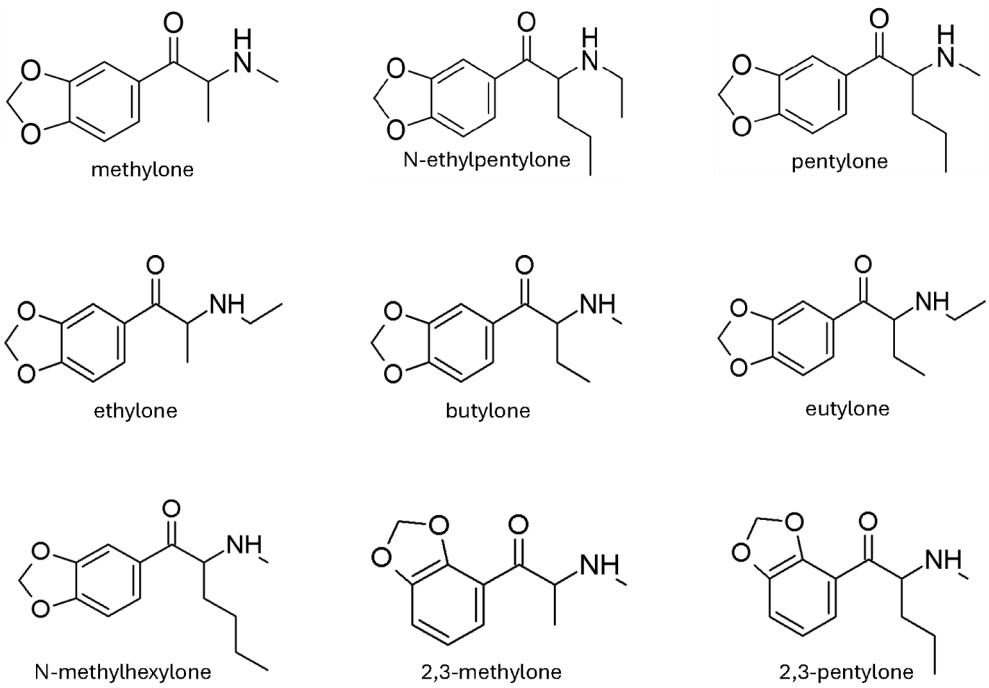

Fig. 1. Structures for Cathinones utilized.

Sample preparation and instrumental settings

Reference materials and case samples at APL were prepared via basic extraction by dissolving sample material in 1 mL of 0.1 mol/L aqueous NaOH solution in a reagent tube, followed by adding 1 mL of chloroform. The reagent tube was closed and shaken on a laboratory agitator for 10 min to allow the apolar free amine form of the drug to dissolve into the chloroform layer. The chloroform layer was transferred into a GC-vial via a pipette filled with glass wool and Hyflo Supercel to both filter and remove residual water from the extract. For pure materials, 4 mg of material was extracted leading to a 4 mg/mL concentration. For tablets, exploratory analysis was used to adjust the amount of material in order to align peak heights with the references standards.

At DFS, the solutions used were previously prepared when needed for casework as reference materials. Thus, the exact concentration and solvents utilized are unknown, although it is suspected that the solutions were methanolic as this is routinely the solvent of choice in this laboratory. Due to limited standard availability, fresh solutions could not be prepared for this study. When not in use, the solutions were stored in a refrigerator at 2–8 °C. In order to compare the methanolic spectra to those prepared via basic extraction at APL, the solutions of methylone, N-ethylpentylone, pentylone, and N-methylhexylone were evaporated to dryness and reconstituted with water. The solution was made alkaline using 1–2 drops of 4 N NaOH solution before extracting into chloroform. The approximate concentration of the base extracted solutions was assessed using GC-FID-MS to ensure sufficient GC-IR signal.

The GC-IR instrument at APL consisted of a 7890B gas chromatograph with a 7693A autoinjector, both from Agilent Technologies (Santa Clara, CA, USA) coupled to a DiscovIR from Spectra Analysis (Marlborough, MA, USA). A 2 μL aliquot was injected into the split injector (5:1 split, 250 °C, 1.5 mL/min Helium constant column flow) and separated on a 30 m HP-5 ms GC column with 320 μm internal diameter and 0.25 μm film thickness. The oven program was as follows: 80 °C initial temperature with a 1.5 min hold, then a ramp of 30 °C/min until 300 °C, which was held for 2 min. The total runtime was 10.83 min. Via a heated transfer line and restrictor (both at 280 °C), the effluent from the GC column was trapped on a ZnSe-disk. This disk was kept at −35 °C in a vacuum chamber of 1.00 * 10^{-5} torr, and rotated at a disk speed of 3 mm/min. FTIR spectra were recorded from 4000 to 700 cm^{-1} at a 4 cm^{-1} resolution using the liquid nitrogen cooled Mercury-Cadmium-Telluride (MCT) detector. The DiscovIR instrument was controlled and spectra were acquired by GRAMS/AI version 9.3.

At DFS, the GC-IR instrument was comprised of a 8890 gas chromatograph with a G4567A autoinjector, both from Agilent Technologies, coupled with a Spectra Analysis DiscovIR. A 1.5 μL injection volume was utilized at a 5:1 split with the injection port set to 270 °C at a constant column Helium flow of 1.8 mL/min. The separation was performed on a 15 m DB-35 ms inert GC column with 250 μm internal diameter and 0.25 μm film thickness. The oven program initiated with a 0.5 min hold at 150 °C, followed by a 15 °C/min ramp to 240 °C, and a subsequent 30 °C/min ramp to 270 °C with a final 1 min hold. This resulted in a total runtime of 8.5 min. The transfer line and restrictor were both heated to 280 °C. The ZnSe-disk was kept at −40 °C in a vacuum chamber of 8.00 * 10^{-5} torr and rotated at a speed of 3 mm/min. The FTIR spectra were recorded from 4000 to 680 cm^{-1} at a 4 cm^{-1} resolution using the liquid nitrogen cooled MCT-A detector. The DiscovIR instrument was controlled and spectra were acquired by DiscovIR version 10.0.3.140.

Data acquisition

To produce the primary dataset, replicate spectra of methylone, N-ethylpentylone, and pentylone were analyzed by 10-fold reanalysis in three different overnight sequences at APL over a three week timeframe. New solutions were prepared each week for the analytical sequence. In between each sequence, the vacuum was vented in order to access and clean the ZnSe disk with acetone. In addition, the detector was re-aligned and the end of the GC column re-positioned slightly above the disk. In several sequences, the final iterations of each substance had to be omitted as the liquid nitrogen stock in the instrument depleted, leading to inadequate cooling of either the disk or the detector. In total, this led to a set of 29 spectra of methylone and 27 spectra each of N-ethylpentylone and pentylone. Additionally, the two casework samples were analyzed in triplicate in a single sequence during the final week.

For all APL chromatograms, the FTIR spectrum of the main peak was manually background corrected by subtracting the average spectrum of

an approximately 0.5 min area next to the chromatographic peak from the average spectrum of the peak itself. The obtained spectra were stored as .spc files for manual library searching and converted to .txt files using GRAMS convert version 9.1 for chemometric modeling.

The methanolic DFS test set was generated over two separate analysis weeks, approximately five weeks apart. The three compounds from the primary dataset (methylone, N-ethylpentylone, and pentylone) were analyzed in triplicate during each analytical session. A fresh methanolic pentylone solution was prepared during the first analytical period and was also analyzed in triplicate, resulting in nine total replicate analyses of methanolic pentylone. N-methylhexylone, a positional isomer of N-ethylpentylone, produced spectra which were visually similar to that of pentylone, and was also analyzed in triplicate during the first analytical period and again approximately one week after the second analytical session. The remaining five cathinone analogs were each analyzed twice, once during each analytical period. The dried down and base extracted solutions were prepared and analyzed approximately nine weeks after the second analytical session. For all spectra, background correction was performed automatically rather than manually. Once again, the spectra were saved as.spc files for library searching and converted to.txt files for chemometric comparison.

Although both instruments were set up to record spectra at 4 cm^{-1} resolution, the resulting data point spacing differed between both sets of spectra. The DFS instrument recorded abundance values every 2 cm^{-1} while the APL instrument provided abundance values every approximately 3.86 cm^{-1}. To account for this discrepancy, an interpolation was performed on the APL spectra using the Numpy library [35] in python.

Data analysis

Manual library search

In order to assess the performance of a chemometric model in comparison with a typical library matching algorithm, a spectral library was created using the standard functionality enclosed in the Data Workup workbook and SpectralID add-on in GRAMS/AI. In a separate dedicated sequence at APL, reference spectra of base extracted methylone, N-ethylpentylone, and pentylone were recorded, baseline subtracted, and stored in this library. These spectra were not part of the primary dataset. In addition, two of the compounds (methylone and N-ethylpentylone) had been previously analyzed using 2 mg/mL methanolic solutions on the same instrument several years prior to the analysis of the primary dataset. Due to instrument availability, a spectrum of pentylone in a methanolic solution was acquired several weeks after the primary dataset. The source of the samples was the same for both libraries and the primary dataset. Both libraries were shared with DFS. The spectra making up the primary dataset, APL casework samples, and DFS standards were searched against these libraries using a first derivative correlation and quality match scores were recorded (ranging from 0 to 1 where 0 indicates a perfect match).

The first derivative correlation library search method was the vendor's suggested standard library search method and was found optimal during preliminary testing. When this method is selected, each spectrum is first mean-centered and the first derivative is subsequently calculated for each spectrum. The resulting spectra for the library and unknown sample are referred to as Lib_i and $Unkn_i$, respectively, and the quality match score (QMS) is calculated using the dot products of the vectors, as shown in Eq. (1) [36]. Library searching at DFS was conducted using the SpectralID add-on of GRAMS/AI version 9.1 which produced the same quality match scores as the searches performed at APL using GRAMS/AI version 9.3.

$$QMS = 1 - \frac{(Lib_i \cdot Unkn_i)^2}{(Lib_i \cdot Lib_i)(Unkn_i \cdot Unkn_i)} \quad \text{where} \quad a \cdot b = \sum_{j=1}^{n} a_j b_j \tag{1}$$

Chemometric analysis

All spectra were analyzed in absorbance mode and normalized to a range of 0–1. Four types of additional preprocessing were investigated: none (original normalized spectra), first derivative, second derivative, and Standard Normal Variate (SNV). In addition, truncating the spectra to only the fingerprint region (1800–700 cm^{-1}) was evaluated. The truncation was performed before the preprocessing. In this manner, only the portion of the spectrum utilized had any influence on the preprocessing method.

Principal Component Analysis (PCA) was performed on the primary dataset after each combination of truncation and preprocessing. As an unsupervised machine learning method, PCA identifies the latent axes in a dataset which represent the highest amount of variance in the data without considering group or class labels. A leave-one-sample-out cross validation was conducted wherein each spectrum was individually removed from the primary dataset, PCA was performed using the remaining spectra, and the held-out sample was subsequently transformed into the resulting vector space. The mahalanobis distances (D_m) were calculated between each held out sample and each compound class, using Eq. (2) where y is the held-out sample, μ is the center of the compound class in question and S is the covariance matrix of the compound class. Distances were calculated using the first three PC axes, covering over 88 % of the total variance.

$$D_m = (y - \mu)^T S^{-1} (y - \mu) \tag{2}$$

Once the preferred combination of truncation/preprocessing was identified, the chemometric model was generated using the entire primary dataset and both the DFS and APL test samples, as well as the library spectra, were preprocessed and projected into the PC space. The mahalanobis distances for each spectrum to each drug class were calculated. This value provided an objective measure of how similar an unknown sample was to a given class. This value was also calculated for the DFS spectra which had no true positive associated with them since their identities were not included in the primary dataset. In this manner, the robustness of the model when faced with an unfamiliar spectrum was assessed. The github repository containing all code is available online [37].

Results and discussion

Visual spectral assessment

A visual inspection of the APL primary dataset spectra (normalized to a range of 0–1) shows substantial similarity between the spectra for the three cathinones. The difference that appears most readily apparent is shown in the full average spectra shown in Fig. 2 and is the decrease in strength in the C–H absorbance between approximately 2800–3000 cm^{-1} for the methylone spectra compared to the other compounds. Additionally, as seen in the truncated average spectra shown in Fig. 3, there appear to be two minor peaks at approximately 1390 cm^{-1} and 1125 cm^{-1} present in the N-ethylpentylone spectra that are not seen in the spectra for the other two compounds. Conversely, the N-ethylpentylone spectra appear to be missing a small peak around 1070 cm^{-1}. In addition, the methylone spectra show a more prominent shoulder peak at approximately 1300 cm^{-1}. However, these differences are minor and would likely not be enough to justify a confident conclusion, particularly when performing a one-to-one visual comparison.

The spectra showed little variation between replicates during a single analytical session, as shown in Figs. S1–S3, but did show some differences from week to week, as seen in the truncated weekly average spectra in Fig. 4. These variations seem to primarily affect peak intensity and could be related to the process of breaking the vacuum to clean the disk and re-position the GC column between analytical sessions which are routine parts of instrument maintenance and use. The spectra

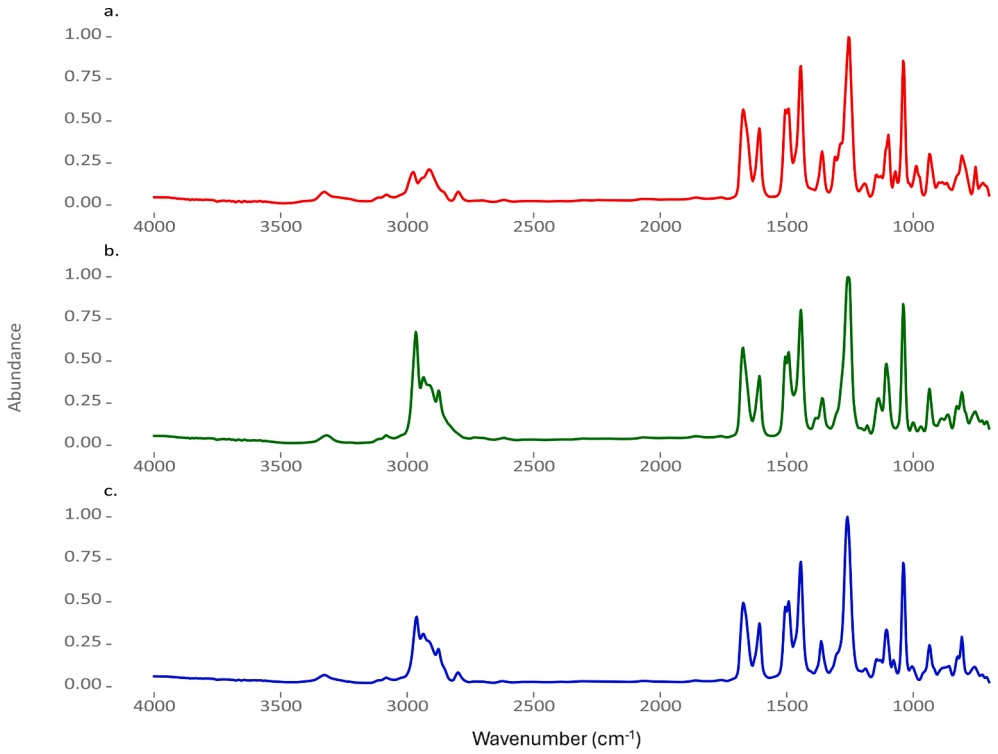

Fig. 2. Full (4000–700 cm^{-1}) APL absorbance average IR spectra for the base extracted primary dataset. a. methylone (n = 29), b. N-ethylpentylone (n = 27), c. pentylone (n = 27).

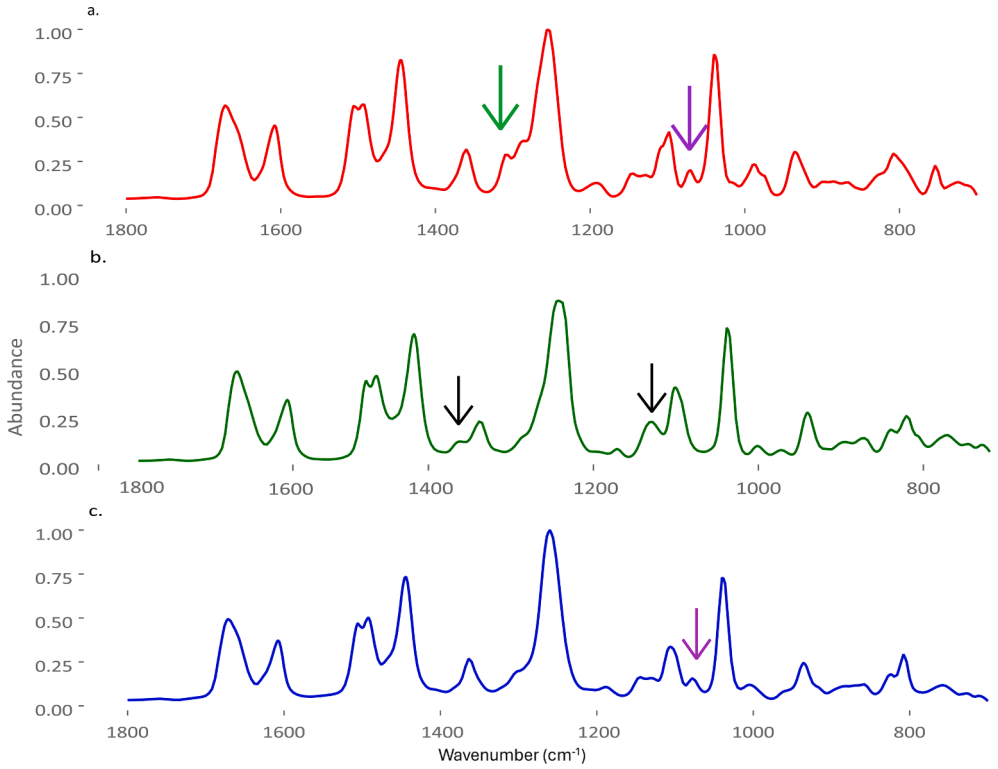

Fig. 3. Truncated (1800–700 cm^{-1}) APL absorbance average spectra for the base extracted primary dataset. a. methylone (n = 29), b. N-ethylpentylone (n = 27), c. pentylone (n = 27). Black arrows at approximately 1390 and 1125 cm^{-1} represent peaks that appear in N-ethylpentylone but seem to be absent from the methylone and pentylone spectra. Purple arrows represent a peak around 1070 cm^{-1} that is present in methylone and pentylone but absent from N-ethylpentylone. The green arrow shows the more prominent shoulder around 1300 cm^{-1} in the methylone spectrum.

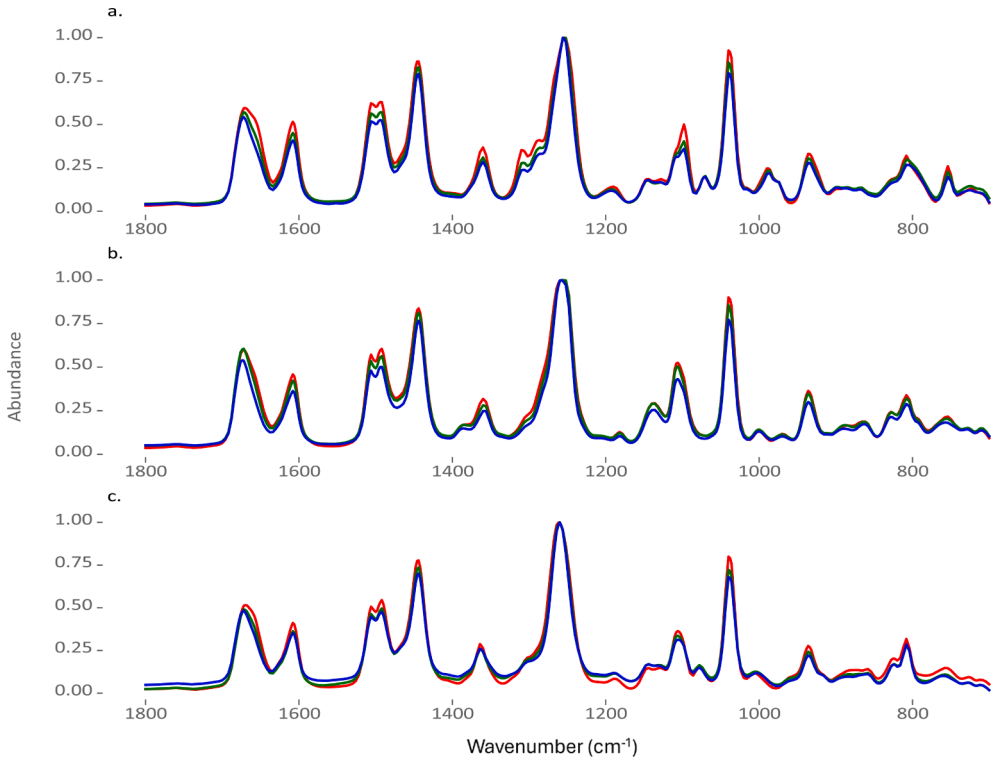

Fig. 4. Truncated (1800–700 cm^{-1}) APL absorbance weekly average spectra for the base extracted primary dataset. a. methylone, b. N-ethylpentylone, c. pentylone. For each compound, the first week is shown in red, second in green, third in blue.

obtained during week three showed the most variation between replicates. The detector on the instrument failed to start when a fourth analysis week was attempted, so this variation may be due to a failing detector. However, no individual spectrum appeared flawed nor would cause an examiner to suspect it could not be used for analysis.

When compared to the base extracted spectra obtained at DFS, (Full spectra shown in Fig. S4, truncated spectra shown in Fig. 5) the small peak at approximately 1390 cm^{-1} is still present in the N-ethylpentylone spectra and missing from the other spectra. However, there appears to be a small hump in the methylone spectra around 1375 cm^{-1} that is not apparent in the APL methylone spectra that could potentially be confused for this small peak. Additionally, while the absorbance decrease for the methylone spectra is still observed around 2800–3000 cm^{-1}, the increased shoulder in the APL methylone spectra around 1300 cm^{-1} is not as prominent in the DFS methylone spectra. The spectra for the six other cathinones are provided in Fig. S5. The 2,3- positional isomers are visually distinct from their 3,4 counterparts, but the remaining cathinones result in spectra that are visually similar to the three cathinones in the primary dataset. Of particular interest is N-methylhexylone which is currently not listed as a controlled substance in the State of Virginia [38], yet produces a spectrum that is nearly visually indistinguishable from the three primary dataset cathinones, particularly pentylone. The average truncated base extracted spectrum of N-methylhexylone is shown in Fig. 5.

Interestingly, the APL library spectra obtained via analysis of the compounds in methanol (Fig. S6), appear to be more visually consistent with the DFS spectra (either base extracted or methanolic) than the APL spectra obtained after performing basic extractions into chloroform. For example, the shoulder near 1300 cm^{-1} is less distinct in the APL methanolic methylone spectrum than in the chloroform spectra, appearing more visually similar in appearance to its counterpart in the DFS methylone spectra. Additionally, the shape of the peaks in the range of approximately 1075–1150 cm^{-1} in the methylone spectra is more similar between the DFS and APL methanolic spectra than it is when comparing the APL base extracted spectra to the methanolic spectrum from the same instrument. This is especially interesting in light of the fact that the methylone source was the same for both APL analyses.

It should be noted that while small differences between the spectra of the different cathinones can be observed and are frequently consistent within spectra obtained using a particular instrument and solvent, they are not always consistent across changes in these parameters. For example, in the APL base extracted spectra, the N-ethylpentylone spectra appear to have a shoulder peak at approximately 1390 cm^{-1} which is not apparent in either the methylone or pentylone spectra, as mentioned previously. This might lead one to believe that this could be a distinguishing feature, yet a similar shoulder is present in the APL methanolic and DFS spectra of methylone. Thus, it is unclear if any small visual differences can be confidently utilized to differentiate the compounds. Many of the potentially distinguishing features are also only discernible when meticulously observing zoomed-in spectra. It is therefore unlikely that they would be detected by a cursory visual inspection unless extreme care was taken.

Even more challenging is the scenario wherein a new compound is encountered and no reference spectra are available for comparison. This is especially apparent when observing the DFS N-methylhexylone spectra. Without appropriate reference spectra, if this compound was encountered as part of a casework exhibit, a visual comparison alone might lead to a misidentification as either N-ethylpentylone or pentylone. The only readily apparent difference seems to be a very low abundance peak at approximately 1000 cm^{-1} in the spectra of both N-ethylpentylone and pentylone which is missing from the spectra of N-methylhexylone. Fortunately, the mass spectral base peak differs for N-methylhexylone and pentylone (m/z 100 and m/z 86, respectively), resulting in a straightforward differentiation. The mass spectra for N-methylhexylone and N-ethylpentylone are more visually similar to one another, as shown in Fig. S7, but do show distinguishable differences in the abundance of $m/z = 44$ and $m/z = 58$. In addition, these compounds are easily separated on an HP-5MS GC column.

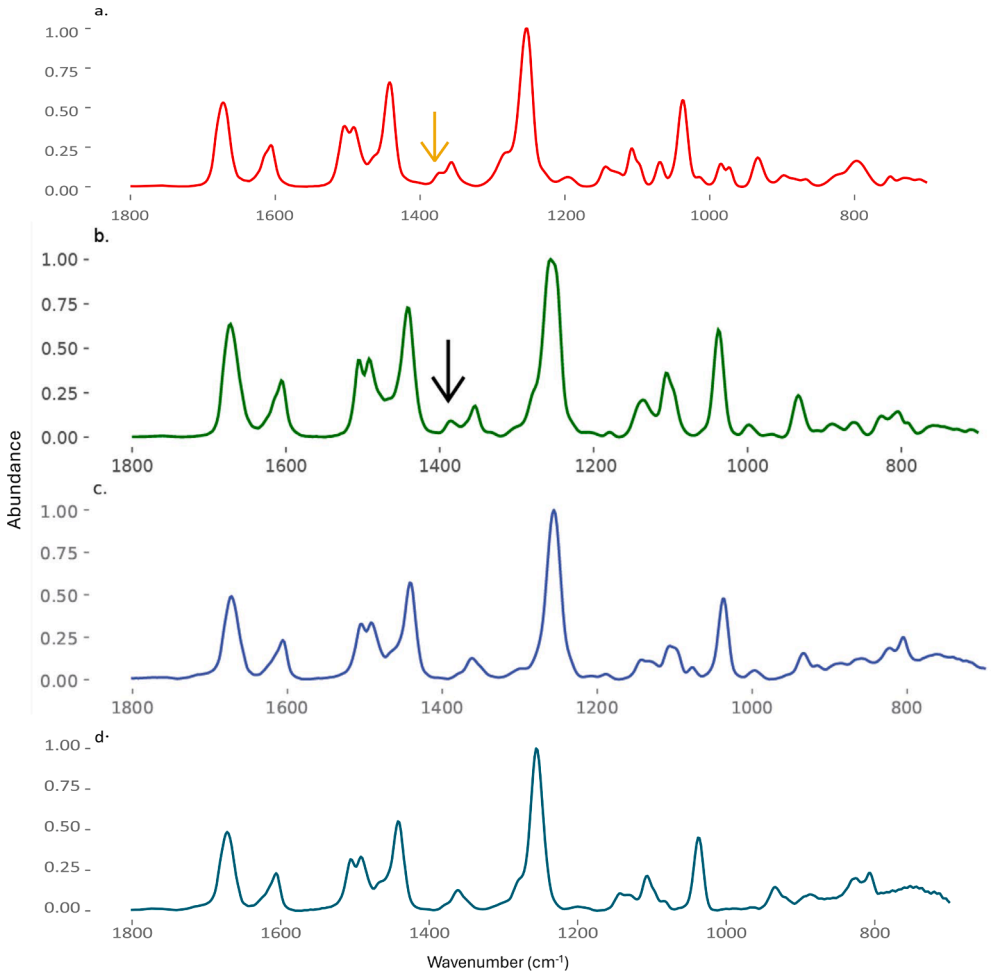

Fig. 5. Truncated (1800–700 cm^{-1}) DFS average absorbance base extracted spectra for a. methylone, b. N-ethylpentylone, c. pentylone. d. N-methylhexylone. The black arrow highlights the peak at approximately 1390 cm^{-1} that is present in the N-ethylpentylone spectra but absent in others. The orange arrow represents a peak around 1375 cm^{-1} that is present in the DFS methylone spectra but absent in the APL methylone spectra and could be confused for the N-ethylpentylone 1390 cm^{-1} peak.

Manual library searching

To assess whether there is a need for chemometric modeling of GC-IR data, the results of a typical library searching algorithm were evaluated. Two library entries were prepared for each of the three cathinones, one as the hydrochloride salt form in methanol and one utilizing a basic extraction into chloroform. These spectra were not part of the primary dataset, although the same base extracted solutions were utilized. Various library search methods are routinely available in the software. In this study, first derivative correlation library searching was applied as this was both the suggested option of the vendor and gave the best performance on a selection of samples during pre-optimization experiments.

Average match scores for the APL primary dataset compared to the

Table 1
Average Match scores with standard deviation for spectra in the primary dataset. (base extracted) compared to methanolic and base extracted methylone, N-ethylpentylone, and pentylone library spectra. Also provided are the minimum and maximum values obtained for each set (in parentheses/italicized). The sets representing the true identity of each compound are shown in bold. The lowest values which correctly represent the correct match are shown in green. Highlighted in red is a maximum value which could have resulted in a misidentification if only methanolic library entries were used and the lowest value were used to make a conclusion rather than setting a threshold for conclusions.

		methylone (library)		N-ethylpentylone (library)		pentylone (library)	
samples	n	base	MeOH	base	MeOH	base	MeOH
methylone	29	**0.053 ± 0.036** *(0.003 - 0.118)*	**0.174 ± 0.069** ***(0.084 - 0.301)***	0.247 ± 0.010 *(0.231 - 0.268)*	0.276 ± 0.048 *(0.220 - 0.364)*	0.192 ± 0.011 *(0.164 - 0.216)*	0.234 ± 0.031 *(0.211 - 0.389)*
N-ethylpentylone	27	0.269 ± 0.023 *(0.232 - 0.297)*	0.254 ± 0.040 *(0.198 - 0.353)*	**0.045 ± 0.03** ***(0.005 - 0.100)***	**0.072 ± 0.032** ***(0.034 - 0.155)***	0.114 ± 0.011 *(0.093 - 0.129)*	0.149 ± 0.012 *(0.125 - 0.165)*
pentylone	27	0.264 ± 0.027 *(0.220 - 0.310)*	0.265 ± 0.03 *(0.234 - 0.316)*	0.173 ± 0.023 *(0.134 - 0.223)*	0.188 ± 0.023 *(0.156 - 0.231)*	**0.032 ± 0.024** ***(0.004 - 0.070)***	**0.057 ± 0.010** ***(0.027 - 0.098)***

two library entries are shown in Table 1. Possible quality match scores range from 0 to 1, with a score of 0 indicating that the compared spectra are identical. The individual match scores for each spectrum are found in Tables S1–S3.

It is immediately apparent that there are considerable differences between the base extracted and methanolic spectra in terms of the match scores obtained when comparing the base extracted primary dataset spectra to each library. The average absolute difference between the match scores based on solvent is shown in Table S4. While the average absolute difference for the methylone primary dataset samples was 0.126, some individual spectra produced match scores which differed by nearly 0.3 between the two solvents. The other cathinones in the primary dataset showed fewer differences based on solvent. The pentylone samples compared to the pentylone library spectra showed the smallest absolute differences, suggesting fewer spectral differences due to the solvent.

Receiver Operator Characteristic (ROC) curves were prepared using the comparison of the primary dataset spectra to the base extracted and methanolic libraries separately, as shown in Fig. 6. This provides visual support for the notion that using the base extracted library spectra for the base extracted primary dataset spectra produced a more stable model. The methanolic library spectra still performed well, but there is a clear decrease in model performance when comparing spectra to a library created using a different sample preparation method.

This difference could possibly be attributed to the well-established keto-enol tautomerization that exists in equilibrium for synthetic cathinones [39]. The equilibrium is shown in Fig. 7. The exact position of the keto-enol equilibrium can be affected by several factors, one of which is the nature of the solvent since the enol tautomer is more likely to form hydrogen bonds intramolecularly, while the keto tautomer may form hydrogen bonds with protic solvents which could stabilize it [40]. Thus, the methanolic solutions may be shifted towards the keto form. However, it is suggested that bulkier α groups may encourage the intramolecular hydrogen bonding and thus stabilize the enol form [40]. As this effect appears to affect methylone samples more severely, it is possible that the slightly bulkier α groups present in both N-ethylpentylone and pentylone may stabilize the enol tautomer, making the keto tautomer less likely to form, even in the presence of a protic solvent such as methanol.

Interestingly, in most analytical sequences the differences became less prominent over the course of the analysis time, with the spectra looking more similar to the methanolic library spectra with each replicate. It is possible that the keto-enol equilibrium shifts over time to be more comparable to its position in methanolic solution. Also worthwhile to note is the observation that when all three cathinones were compared to the N-ethylpentylone library, the lower (better) match scores were typically observed when comparing to the base extracted spectrum in weeks 1 and 2, but the methanolic spectrum in week 3. This is shown in Table S2. As new sample solutions were prepared for each analytical sequence, it is unclear why this would be the case and may suggest that the equilibrium is not as predictable as it seems. This also emphasizes

Fig. 7. The equilibrium between the keto-enol tautomers of cathinone compound, methylone used for illustrative purposes. The keto tautomer is shown on the left, while the enol form is shown on the right.

the difficulty associated with using a singular reference spectrum for comparison as is done with library matching methods.

It is unlikely that the differences are due to degradation as the solutions were re-analyzed via GC–MS after the GC-IR analysis and no degradation was noted. Furthermore, it is unlikely that the differences are due to the salt form of the drug being present in the methanolic solutions. While the salt form can affect chromatographic performance, it has previously been shown that when drugs are injected into a GC-IR as salts, they elute in their base form [7].

These differences in spectra when utilizing a different solvent or sample preparation method are especially important to notice as there were several base extracted methylone spectra in the primary dataset that would have been misidentified as pentylone if only the methanolic library spectra were available. Interestingly, this observation only occurred during the first analysis week.

The library match scores for the triplicate analyses of two APL casework samples are shown in Table 2. For both samples, the lowest match scores (indicating a better match quality) correctly identified the substance in the case sample and are below the thresholds indicated by the ROC curves shown in Fig. 6 for both the base extracted and methanolic libraries. The range of match scores obtained for the incorrect compounds are over these thresholds, supporting the true negative results for these compounds. However, these thresholds are shown to be incompatible with spectra obtained from another instrument/laboratory. The average match scores obtained for DFS samples are shown in Table 3 and the individual match scores are listed in Table S5. The match scores obtained for the true positive comparisons are much higher for the DFS samples than they are for the APL samples, and are frequently at or above the thresholds determined by the ROC curves. This suggests that typical library match results can suffer when comparing spectra obtained using a different instrument. In fact, if the spectra were classified solely according to the library match which provided the lowest match score, the DFS pentylone spectra would be misidentified as N-ethylpentylone.

Interestingly, the base extracted DFS samples generated lower match scores when compared to the methanolic library than the base extracted library. This may be due to the nature of these solutions (likely methanolic) which had been stored for a period of time before being dried down and reconstituted in water for the basic extraction and subsequent immediate analysis. As the APL results showed that the primary dataset typically showed less solvent differences overtime, it may be that the

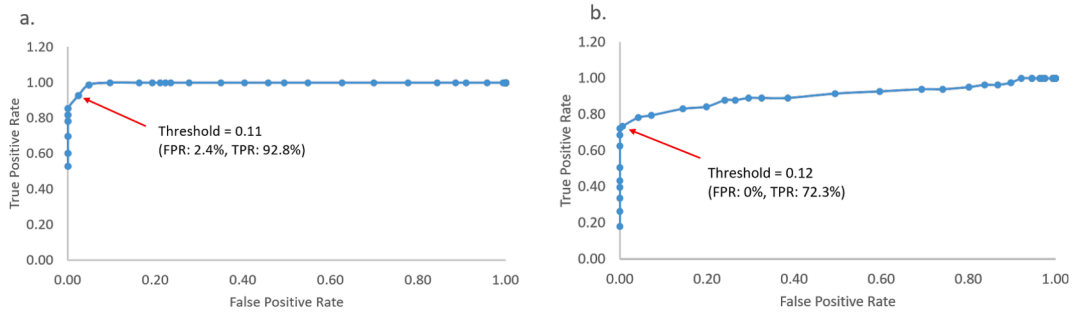

Fig. 6. ROC curves generated using a. base extracted library spectra, b. methanolic library spectra. The thresholds which produced the approximate upper left corners of the curves are provided.

Table 2
Match scores for base extracted case samples analyzed at APL compared to library spectra for methanolic and base extracted methylone, N-ethylpentylone, and pentylone. The lowest value for each sample is shown in bold and green to highlight that a true positive association was observed.

Case Sample - replicate	Substance	methylone (library)		N-ethylpentylone (library)		pentylone (library)	
		base	*MeOH*	*base*	*MeOH*	*base*	*MeOH*
1 - 1	pentylone	0.263	0.240	0.154	0.155	**0.029**	0.059
1 - 2		0.291	0.251	0.196	0.177	**0.052**	0.068
1 - 3		0.295	0.260	0.211	0.187	**0.057**	0.080
2 - 1	N-ethylpentylone	0.287	0.247	0.054	**0.050**	0.124	0.161
2 - 2		0.280	0.256	**0.043**	0.060	0.124	0.161
2 - 3		0.283	0.221	0.072	**0.046**	0.122	0.158

Table 3
Average Match scores with standard deviation for DFS spectra for the three cathinones of interest compared to methanolic and base extracted methylone, N-ethylpentylone, and pentylone APL library spectra. Also provided are the minimum and maximum values obtained for each set (in parentheses/italicized). Correctly classified averages which are below the thresholds determined by the ROC curves are shown in green while misclassified averages are shown in red. The averages representing the correct compound identity are highlighted in bold.

Samples	Sample Preparation	n	methylone (library)		N-ethylpentylone (library)		pentylone (library)	
			base	*MeOH*	*base*	*MeOH*	*base*	*MeOH*
methylone	Methanol	6	**0.367 ± 0.010** ***(0.357 - 0.379)***	**0.115 ± 0.004** ***(0.111 - 0.119)***	0.372 ± 0.011 *(0.361 - 0.386)*	0.225 ± 0.002 *(0.222 - 0.228)*	0.401 ± 0.008 *(0.391 - 0.410)*	0.440 ± 0.008 *(0.430 - 0.449)*
	Base extraction	3	**0.411 ± 0.001** ***(0.410 - 0.412)***	**0.123 ± 0.002** ***(0.121 - 0.125)***	0.413 ± 0.001 *(0.412 - 0.413)*	0.237 ± 0.001 *(0.236 - 0.238)*	0.439 ± 0.002 *(0.437 - 0.440)*	0.479 ± 0.002 *(0.477 - 0.480)*
N-ethylpentylone	Methanol	6	0.348 ± 0.015 *(0.323 - 0.368)*	0.319 ± 0.010 *(0.303 - 0.328)*	**0.180 ± 0.014** ***(0.159 - 0.203)***	**0.123 ± 0.006** ***(0.113 - 0.129)***	0.284 ± 0.016 *(0.257 - 0.301)*	0.311 ± 0.019 *(0.279 - 0.331)*
	Base extraction	3	0.395 ± 0.004 *(0.392 - 0.400)*	0.275 ± 0.004 *(0.271 - 0.279)*	**0.244 ± 0.006** ***(0.239 - 0.251)***	**0.109 ± 0.001** ***(0.108 - 0.110)***	0.320 ± 0.004 *(0.317 - 0.324)*	0.350 ± 0.004 *(0.347 - 0.355)*
pentylone	Methanol	9	0.331 ± 0.014 *(0.312 - 0.348)*	0.268 ± 0.017 *(0.248 - 0.291)*	0.245 ± 0.013 *(0.226 - 0.262)*	0.172 ± 0.010 *(0.161 - 0.185)*	**0.201 ± 0.010** ***(0.183 - 0.212)***	**0.236 ± 0.012** ***(0.214 - 0.248)***
	Base extraction	3	0.485 ± 0.002 *(0.483 - 0.486)*	0.205 ± 0.003 *(0.203 - 0.208)*	0.412 ± 0.004 *(0.408 - 0.415)*	0.187 ± 0.004 *(0.183 - 0.190)*	**0.347 ± 0.003** ***(0.343 - 0.349)***	**0.387 ± 0.002** ***(0.384 - 0.388)***

DFS samples had already reached a stable equilibrium and additional preparation did not cause a significant shift. This may be a concern for casework samples which are typically analyzed shortly after sample preparation.

The match scores for the six additional cathinones analyzed at DFS are provided in Table S6. The 2,3-isomers of both methylone and pentylone gave extremely high match scores to all library spectra, indicating little to no spectral similarity despite the positional isomerism. This illustrates that IR spectra are strongly affected by the position of functional groups on an aromatic ring. IR spectra of drug compounds seem to be more similar when the only structural differences are related to aliphatic chain length instead. This finding has also been observed by Salerno et al. [19] and Kranenburg et al. [20]. For example, the structure of eutylone only differs from that of N-ethylpentylone by one carbon chain length. Thus, the eutylone spectra produced match scores when compared to the methanolic N-ethylpentylone library spectrum that were lower than those obtained even when comparing DFS pentylone spectra to both of the APL pentylone library spectra. This re-emphasizes how erroneous conclusions are easily drawn if library matches alone are relied upon, particularly if using libraries generated on a different instrument. This calls into question whether the typical practice of utilizing shared IR libraries is acceptable. To fully access the orthogonal selectivity of the instrument (next to GC–MS), dedicated instrument-specific libraries would need to be created or multivariate data analysis methods would need to be applied as is explored next.

Chemometric analysis

After PCA was performed on the primary dataset using all combinations of truncation and preprocessing, the data was projected into the vector space represented by the first two resulting principal components. The generated score plots for the full spectra are seen in Fig. 8, and the score plots for the truncated data are shown in S8. The loadings for the first two PCs for the models created using the full spectra are shown in Figs. S9 and S10, and in Figs. S11 and S12 for the truncated spectra.

It is clear from a visual inspection of the PCA score plots that even with minimal (normalization) preprocessing, there are inherent differences that lead to compound separation. However, additional preprocessing does help to remove instrumental variance which allows the structural differences to stand out and further separate the compounds from one another. This is supported by the mahalanobis distances when a leave-one-sample-out cross validation was performed. For each excluded spectrum, the mahalanobis distance was calculated to each compound cluster in PC space, using the first three principal components. For all combinations of truncation and preprocessing, only PCA performed on the full original spectra resulted in 1 misclassification. All other combinations resulted in 100 % accuracy based on assigning the left-out sample to the compound cluster which yielded the lowest mahalanobis distance. The maximum distance obtained when comparing a sample to its correct compound cluster was noted for each preprocessing combination, as well as the minimum distance obtained

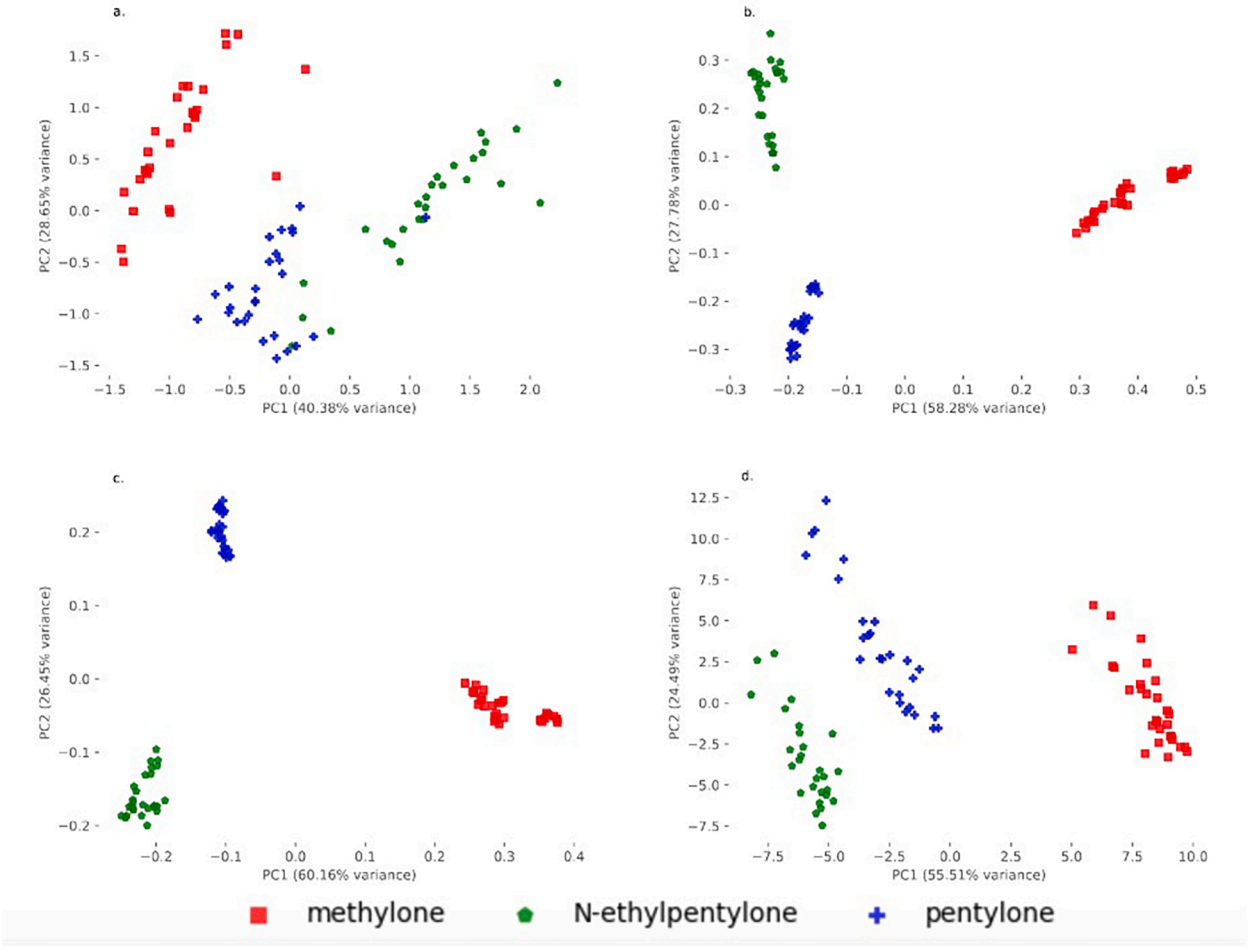

Fig. 8. PCA Score plots of 0th (original) (a.), 1st (b.), 2nd (c.) derivative and SNV (d.) spectra using the primary dataset. Full spectra used. The proportion of variance described by each principal component is shown on the respective axis.

between a sample and either of the incorrect compound clusters. The highest difference in these two values was obtained when the full second derivative spectra were used. This is shown in Table 4. Thus, this method was chosen for further exploration.

The spectra used to create the library entries at APL, the APL case-work samples, and the samples analyzed at DFS were utilized as test sets to assess the performance of the chemometric model. When transformed into the PC space generated using the second derivative spectra of the full primary (base-extracted) dataset, the score plots are seen in Fig. 9. A visual inspection of the score plot in Fig. 9a shows that the base extracted APL methylone sample, as well as all APL N-ethylpentylone and pentylone library and case samples are easily attributed to their correct compound cluster. In Fig. 9b it is seen that the DFS N-ethyl-pentylone and pentylone samples of both solvent types are more similar to the correct cluster than they are to the other compounds. This is an improvement over the library match in which the DFS pentylone samples were misidentified as N-ethylpentylone. Conversely, both the APL methanolic methylone spectrum and all of the DFS methylone samples

Table 4
Comparison of Mahalanobis distances (D_m) between maximum distance observed from samples to their correct group and the minimum distance observed from samples to their incorrect groups when performing a leave-one-sample-out validation. The highest difference is shown in green.

	Variance in 3 PCs	Max D_m - correct	Min D_m - Incorrect	Difference
Original - Full	88.3%	35	15	-20
Original - Truncated	88.6%	29	62	33
First - Full	95.5%	11	1260	1249
First - Truncated	94.9%	10	1294	1284
Second - Full	94.8%	14	1926	1912
Second - Truncated	95.0%	14	1423	1408
SNV - Full	88.0%	24	57	33
SNV - Truncated	89.1%	21	68	47

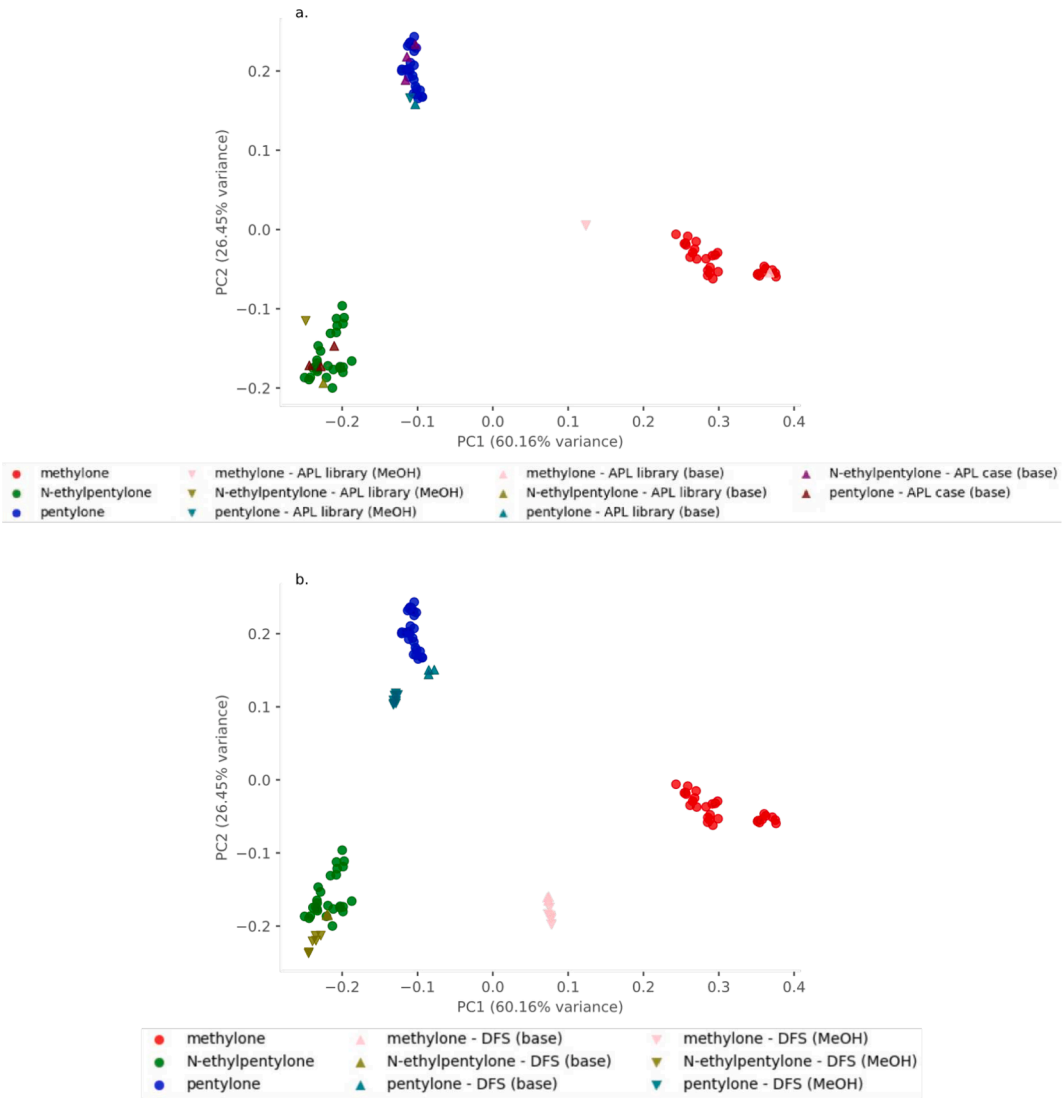

Fig. 9. PCA Score plots of full second derivative spectra projecting APL (a.) and DFS, (b.) test samples into the PCA space generated using the primary dataset. The proportion of variance described by each principal component is shown on the respective axis.

are visually removed from the methylone cluster.

When mahalanobis distances are calculated using the first three principal components, as shown in Table 5, it is once again seen that the base extracted DFS pentylone samples are misidentified as N-ethylpentylone when classifying the samples to the class which produced the smallest mahalanobis distance. This misidentification does not occur if the mahalanobis distances are calculated using only the first two principal components, as seen in Table S7 and supported by the visual examination of the two-dimensional PCA plots. Additionally, each DFS sample resulted in much higher mahalanobis distances than those obtained using the APL samples when three principal components are used, but the distances decrease substantially for the N-ethylpentylone and pentylone samples when only the first two are used. This may suggest that there is a benefit to restricting the calculation to two principal components; however more samples would be necessary to investigate this result. The PC3 loadings (from the full second derivative spectra), as shown in Fig. S13, are heavily influenced by the strong absorbance around 1250 cm^{-1} wavenumbers. This peak seems to be slightly more broad in the APL spectra when compared to the DFS spectra which may help explain this difference.

It is worth noting that although the visual examination of the score plot shows that the APL methanolic methylone library spectrum is somewhat removed from the main methylone cluster, the mahalanobis distances using both two and three principal components are of a similar scale to those obtained during the leave-one-sample-out cross validation. This suggests that within a single instrument, chemometrics handles solvent differences better than the library matching method. This is unsurprising, as condensing subtle spectral differences to a single parametric match score does not make optimal use of the spectral information. Furthermore, when the PCA score plot is visualized by color-coding the analysis weeks, as shown in Fig. 10, it is seen that there are some weekly shifts. Thus, this sample may be further removed due to both time and solvent differences. Additional work should be done exploring these variations using more spectra taken in a similar time period. However, despite this observation, the DFS replicates that were obtained over a total of approximately 15 weeks are much more internally consistent and seem to show differences based on sample preparation methods more than time period. While inter-system conclusions are not yet reliable, the reproducibility within a single instrument suggests improvement over the current library match model, particularly with respect to changes in solvent and over time.

In Fig. 11, the DFS spectra of compounds not included in the primary dataset are transformed into the PCA space. The mahalanobis distances obtained using two and three principal components are shown in Tables S8 and S9, respectively. Some compounds, butylone in particular, produce mahalanobis distances on a similar scale to those generated by

Table 5
Mahalanobis distances (D_m) between test samples and the compounds in the primary dataset using three principal components. When n > 1, the average and standard deviation are provided. The distances representing the correct identity are highlighted in bold. When the smallest distances are encountered for the correct compound cluster, the result is shown in green. Otherwise, the result is shown in red.

Samples	Lab	Sample Preparation	n	methylone	N-ethylpentylone	pentylone
methylone	DFS	Base extraction	3	**290 ± 8**	3321 ± 43	17078 ± 99
		Methanol	6	**363 ± 23**	3532 ± 90	17402 ± 191
	APL	Base extraction (library)	1	**8.4**	3134	24611
		Methanol (library)	1	**19**	1462	13545
N-ethylpentylone	DFS	Base extraction	3	2344 ± 35	**151 ± 8**	3438 ± 43
		Methanol	6	3128 ± 130	**109 ± 32**	3125 ± 189
	APL	Base extraction (case)	3	2962 ± 311	**3.7 ± 1.9**	2277 ± 61
		Base extraction (library)	1	3997	**15**	1785
		Methanol (library)	1	2256	**12**	2412
pentylone	DFS	Base extraction	3	890 ± 34	368 ± 24	**1612 ± 95**
		Methanol	9	2127 ± 156	932 ± 61	**334 ± 56**
	APL	Base extraction (case)	3	2672 ± 27	2308 ± 258	**5.5 ± 5.6**
		Base extraction (library)	1	3149	2116	**3.5**
		Methanol (library)	1	3170	2228	**4.9**

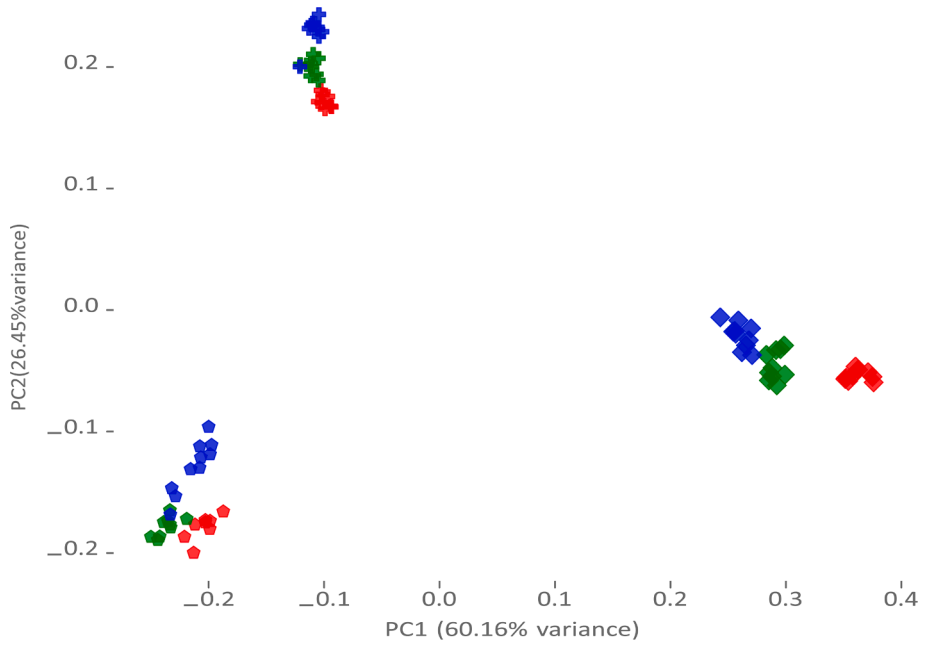

Fig. 10. APL base extracted primary dataset using full second derivative spectra in PCA space, showing differences from week to week. Week 1 is shown in red, week 2 in green, and week 3 in blue. Methylone samples are represented by a diamond, N-ethylpentylone by a pentagon, and pentylone by a cross. The proportion of variance described by each principal component is shown on the respective axis.

the DFS spectra of compounds that are represented by the primary dataset. It is the intent that a chemometric model would only be utilized once other data (library search results or GC–MS, for example) support that an unknown sample is one of the compounds included in the model. Of course, when compounds are so similar, that fact may not always be confidently established. Of specific concern are the N-methylhexylone samples when comparing their location in Fig. 11 to the DFS pentylone samples in Fig. 9. These two compounds seem to be similarly located in two-dimensional PCA space (as generated using the APL primary dataset) and even show a similar visual relationship between the two sample preparation methods. This reiterates that for similar compounds, additional orthogonal methods are necessary to arrive at a confident identification.

Due to instrument and reference material availability, it was not feasible for this study to obtain APL spectra for the cathinones analyzed at DFS which were not included in the primary dataset. This would be a worthy avenue of investigation as it would provide an additional measure of whether chemometrics is better suited to handling novel

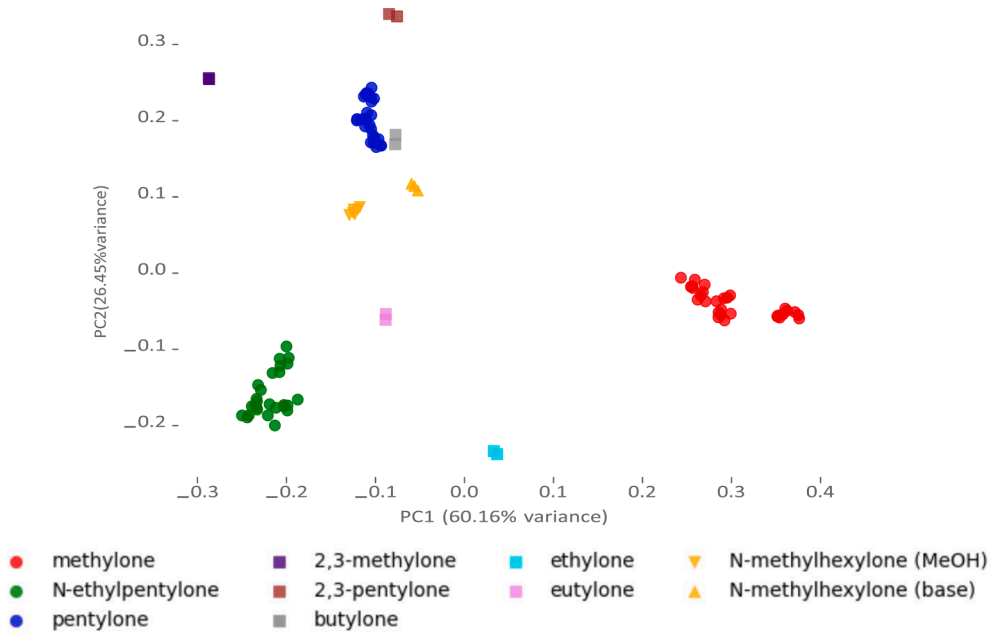

Fig. 11. PCA Score plot of full second derivative spectra projecting DFS samples whose identity are not included in the primary dataset onto the PCA space generated using primary (APL base extracted) dataset. The proportion of variance described by each principal component is shown on the respective axis.

compounds. This would also allow for the development of a method with which to better assess whether an unknown compound is accurately represented by the model.

Conclusions and next steps

The results of this study show that although GC-IR data is highly selective and orthogonal to GC–MS data, it is not as robust and reproducible, showing substantial variations over time and as a function of instrument and even sample preparation method. This complicates the use of shared spectral libraries as is common for GC–MS. However, these challenges can in part be mitigated using chemometrics (multivariate data analysis methods). Using shared libraries is sub-optimal and could even lead to misidentifications, a finding that could have significant repercussions for the field.

We propose that the challenges observed in this study could be addressed with improvements to the chemometric model. Utilizing second derivative spectra served to mitigate a substantial amount of spectral variations that arose due to differences in sample preparation and instrumentation. Through utilization of multiple instrument systems, addition of more spectra, and exploration of supervised chemometric techniques such as LDA, instrumental and methodological effects may be further minimized. This could lead to robust chemometric models that could be broadly applied and would not require frequent gathering of model data.

Although one of the primary benefits to the utilization of chemometric methods of data analysis is the improved objective measures that are available for the forensic scientist to use to form a conclusion, it is also clear that the resulting visual comparison is substantially simpler than a meticulous inspection of the spectra themselves. It is not intended that chemometrics will ever render an expert inspection of chemical spectra irrelevant. Rather, the addition of PCA plots that could both supplement the conclusion and also provide an easier visual aid to present in court to a jury is an added beneficial byproduct of the method.

As with any forensic analytical scheme, conducting additional appropriate instrumental examinations will improve the confidence in the final compound identification. It is therefore not suggested that incorporating chemometrics into the analysis of GC-IR spectra will replace GC–MS. Rather, our goal was to evaluate whether the discriminating power and robustness of the GC-IR could be enhanced through the addition of chemometric techniques. In this manner, an expert who utilizes the GC-IR in an analytical scheme will possess additional objective data to support a final conclusion.

CRediT authorship contribution statement

Jennifer L. Bonetti: Writing – original draft, Visualization, Methodology, Formal analysis, Conceptualization. **Ruben F. Kranenburg:** Writing – review & editing, Investigation. **Stephen Hokanson:** Investigation. **Matthew Pothier:** Investigation. **Saer Samanipour:** Methodology, Conceptualization. **Arian C. van Asten:** Writing – review & editing, Methodology, Conceptualization.

Declaration of competing interest

The authors declare that they have no known competing financial interests or personal relationships that could have appeared to influence the work reported in this paper.

Appendix A. Supplementary data

Supplementary data to this article can be found online at https://doi.org/10.1016/j.forc.2024.100619.

Data availability

The data underlying this study are openly available in Figshare at https://doi.org/10.6084/m9.figshare.27607134.

References

[1] UNODC, World Drug Report 2023, 2023, https://www.unodc.org/unodc/en/data-and-analysis/world-drug-report-2023.html [accessed: 2024-06-28].
[2] M. Verhoeven, J. Bonetti, R. Kranenburg, A. van Asten, Chemical identification and differentiation of positional isomers of novel psychoactive substances – a comprehensive review, *TrAC Trends Anal. Chem.* 166 (2023) 117157.
[3] S. Aslani, D.W. Armstrong, High information spectroscopic detection techniques for gas chromatography, *J. Chromatogr. A* 1676 (2022) 463255.

[4] M.-M. Blum, H. John, Historical perspective and modern applications of attenuated total reflectance – Fourier transform infrared spectroscopy (ATR-FTIR), *Drug Test. Anal.* 4 (2012) 298–302.
[5] A. Lanzarotta, Analysis of forensic casework utilizing infrared spectroscopic imaging, *Sensors* 16 (2016).
[6] A.V. Ewing, S.G. Kazarian, Infrared spectroscopy and spectroscopic imaging in forensic science, *Analyst* 142 (2017) 257–272.
[7] R. Shipman, T. Conti, T. Tighe, E. Buel, Forensic drug identification by gas chromatography - infrared spectroscopy, 2013, [Grant Report Accessed: 2024-06-28].
[8] T. Awad, T. Belal, J. DeRuiter, K. Kramer, C.R. Clark, Comparison of GC–MS and GC–IRD methods for the differentiation of methamphetamine and regioisomeric substances, *Forensic Sci. Int.* 185 (2009) 67–77.
[9] A.D. Winokur, L.M. Kaufman, J.R. Almirall, Differentiation and identification of fentanyl analogues using GC-IRD, *Forensic Chem.* 20 (2020) 100255.
[10] K.M. Abdel-Hay, T. Awad, J. DeRuiter, C.R. Clark, Differentiation of methylenedioxybenzylpiperazines (MDBPs) and methoxymethylbenzylpiperazines (MMBPs) By GC-IRD and GC–MS, *Forensic Sci. Int.* 210 (2011) 122–128.
[11] K. Ferguson, S.L. Tupik, H. Haddad, J. Perr, M. Gilbert, R. Newman, J. Almirall, Utility of gas chromatography infrared spectroscopy (GC-IR) for the differentiation of positional isomers of fentanyl related substances, *Forensic Chem.* 29 (2022) 100425.
[12] K. Ferguson, J. Perr, S. Tupik, M. Gilbert, R. Newman, A. Winokur, I. Vallejo, S. Hokanson, M. Pothier, B. Knapp, M. Icard, K. Kramer, J. Almirall, An interlaboratory study to evaluate the utility of gas chromatography-mass spectrometry and gas chromatography-infrared spectroscopy spectral libraries in the forensic analysis of fentanyl-related substances, *J. Forensic Sci.* 68 (2023) 1504–1519.
[13] T. Belal, T. Awad, J. DeRuiter, C.R. Clark, GC–IRD methods for the identification of isomeric ethoxyphenethylamines and methoxymethcathinones, *Forensic Sci. Int.* 184 (2009) 54–63.
[14] M. Almaghrabi, Y. Abiedalla, M. Dhanasakaran, J. DeRuiter, C. Randall Clark, GC–MS and GC–IR of regioisomeric 4-N-bromodimethoxybenzyl derivatives of 3trifluoromethylphenylpiperazine, *Forensic Chem.* 29 (2022) 100416.
[15] Y. Abiedalla, A.J. Almalki, J. DeRuiter, C.R. Clark, GC–MS and GC–IR analysis of substituted N-benzyl 4-bromo-2,5-dimethoxyphenylisopropylamines, *Forensic Chem.* 24 (2021) 100326.
[16] A. Lanzarotta, L. Lorenz, S. Voelker, T.M. Falconer, J.S. Batson, Forensic drug identification, confirmation, and quantification using fully integrated gas chromatography with Fourier transform infrared and mass spectrometric detection (GC-FT-IR-MS), *Appl. Spectrosc.* 72 (2018) 750–756.
[17] H.S. Lee, H. Koh, S. Tan, B. Goh, R. Lim, J. Lim, T.A. Yap, Identification of closely related new psychoactive substances (NPS) using solid deposition gas-chromatography infra-red detection (GC–IRD) spectroscopy, *Forensic Sci. Int.* 299 (2019) 21–33.
[18] M. Dybek, J. Wallach, P.V. Kavanagh, T. Colestock, N. Filemban, G. Dowling, F. Westphal, S.P. Elliott, A. Adejare, S.D. Brandt, Syntheses and analytical characterizations of the research chemical 1-[1-(2-fluorophenyl)-2-phenylethyl] pyrrolidine (fluorolintane) and five of its isomers, *Drug Test. Anal.* 11 (2019) 1144–1161.
[19] T.M.G. Salerno, P. Donato, G. Frison, L. Zamengo, L. Mondello, Gas chromatography—Fourier transform infrared spectroscopy for unambiguous determination of illicit drugs: a proof of concept, *Front. Chem.* 8 (2020).
[20] R.F. Kranenburg, L.I. Stuyver, R. de Ridder, A. van Beek, E. Colmsee, A.C. van Asten, Deliberate evasion of narcotic legislation: trends visualized in commercial mixtures of new psychoactive substances analyzed by GC-solid deposition-FTIR, *Forensic Chem.* 25 (2021) 100346.
[21] A. Martyna, G. Zadora, T. Neocleous, A. Michalska, N. Dean, Hybrid approach combining chemometrics and likelihood ratio framework for reporting the evidential value of spectra, *Anal. Chim. Acta* 931 (2016) 34–46.
[22] E.L. Stuhmer, V.L. McGuffin, R.W. Smith, Discrimination of seized drug positional isomers based on statistical comparison of electron-ionization mass spectra, *Forensic Chem.* 20 (2020).
[23] J. Bonetti, Mass spectral differentiation of positional isomers using multivariate statistics, *Forensic Chem.* 9 (2018) 50–61.
[24] J.T. Davidson, G.P. Jackson, The differentiation of 2,5-dimethoxy-N-(Nmethoxy-benzyl)phenethylamine (NBOMe) isomers using GC retention indices and multivariate analysis of ion abundances in electron ionization mass spectra, *Forensic Chem.* 14 (2019).
[25] R.F. Kranenburg, D. Peroni, S. Affourtit, J.A. Westerhuis, A.K. Smilder, A.C. van Asten, Revealing hidden information in GC-MS spectra from isomeric drugs: Chemometrics based identification from 15 eV and 70 eV EI mass spectra, *Forensic Chem.* 18 (2020).
[26] J.L. Bonetti, R.F. Kranenburg, E. Schoonderwoerd, S. Samanipour, A.C. van Asten, Instrument-independent chemometric models for rapid, calibration-free NPS isomer differentiation from mass spectral GC-MS data, *Forensic Sci. Int.* 348 (2023) 111650.
[27] Z.R. Roberson, H.C. Gordon, J.V. Goodpaster, Instrumental and chemometric analysis of opiates via gas chromatography-vacuum ultraviolet spectrophotometry (GCVUV), *Anal. Bioanal. Chem.* 412 (2020) 1123–1128.
[28] M. Quinn, T. Brettell, M. Joshi, J. Bonetti, L. Quarino, Identifying PCP and four PCP analogs using the gold chloride microcrystalline test followed by raman microspectroscopy and chemometrics, *Forensic Sci. Int.* 307 (2020) 110135.
[29] J. Bonetti, S. Samanipour, A.C. van Asten, Utilization of machine learning for the differentiation of positional NPS isomers with direct analysis in real time mass spectrometry, *Anal. Chem.* 94 (2022) 5029–5040.
[30] E. Deconinck, C. Duchateau, M. Balcaen, L. Gremeaux, P. Courselle, Chemometrics and infrared spectroscopy - A winning team for the analysis of illicit drug products, *Rev. Anal. Chem* 41 (2022) 228–255.
[31] M. Praisler, I. Dirinck, J. Van Bocxlaer, A. De Leenheer, D. Massart, Identification of novel illicit amphetamines from vapor-phase FTIR spectra — a chemometrical solution, *Talanta* 53 (2000) 155–170.
[32] M. Praisler, I. Dirinck, J. Van Bocxlaer, A. De Leenheer, D. Massart, Computer-aided screening for hallucinogenic and stimulant amphetamines with gas chromatography-fourier transform infrared spectroscopy (GC-FTIR), *J. Anal. Toxicol.* 25 (2001) 45–56.
[33] M. Praisler, I. Dirinck, J. Van Bocxlaer, A. De Leenheer, D. Massart, Pattern recognition techniques screening for drugs of abuse with gas chromatography–Fourier transform infrared spectroscopy, *Talanta* 53 (2000) 177–193.
[34] S. Gosav, M. Praisler, J. Van Bocxlaer, A. De Leenheer, D. Massart, Class identity assignment for amphetamines using neural networks and GC–FTIR data, Spectrochim. Acta Part A: Mol. Biomol. Spectroscopy 64 (2006) 1110–1117, 34th Colloquium Spectroscopicum Internationale.
[35] C.R. Harris, et al., Array programming with NumPy, *Nature* 585 (2020) 357–362.
[36] Inc., T. F. S. Help topics: correlation algorithm and first derivative correlation algorithm, 2009.
[37] J. Bonetti, GCIR Forensic Chemistry, 2024, https://github.com/JBonetti2790/GCIR_Forensic_Chemistry [accessed: 2024-10-24].
[38] https://law.lis.virginia.gov/vacode/title54.1/chapter34/section54.1-3446/, [Accessed: 2024 - 08 - 13].
[39] S. Kerrigan, M. Savage, C. Cavazos, P. Bella, Thermal degradation of synthetic cathinones: implications for forensic toxicology, *J. Anal. Toxicol.* 10 (2016) 1–11.
[40] P.E. Allegretti, M. de las Mercedes Schiavoni, E.A. Castro, J.J. Furlong, Tautomeric equilibria studies by mass spectrometry, World J. *Chem.* 2 (2007) 26–62.